Forschung im Ingenieurwesen (2025)89:7
https://doi.org/10.1007/s10010-025-00799-x

ORIGINALARBEITEN/ORIGINALS

Influence of hydrodynamic planetary journal bearings on the NVH-behavior of wind turbines

Moataz Sabry[1] · Georg Jacobs[1] · Thomas Decker[1] · Wilhelm Schünemann[1] · Ralf Schelenz[1]

Received: 17 September 2024 / Accepted: 30 January 2025

Abstract

The growth of the wind energy sector is confronted with stringent noise regulations, particularly concerning tonal noises from wind turbines (WTs). These tonal noises, originating from drivetrain vibrations such those caused by gear meshing, are transmitted as structure-borne sound through the WT and ultimately emerge into the surrounding environment as sound emissions. Given that tonal noises are irritating to humans, there is a need for early-stage noise, vibration, and harshness (NVH) mitigation.

Recently, a trend has emerged towards replacing planetary rolling bearings (PRBs) with planetary journal bearings (PJBs) in the gearboxes of WT drivetrains. This shift offers several advantages, including reduced installation space, increased reliability, and improved vibration reduction, the latter being especially important for complying with noise regulations. Thus, this paper aims to analyze the impact of using PJBs on the NVH behavior of WTs. To achieve this, the dynamic behavior of a generic 5 MW WT under nominal operational conditions is simulated using a multi-body simulation (MBS) model. The findings of this study indicate significant potential for enhanced noise mitigation through the adoption of PJBs, with the bearing main parameters playing a role in the damping characteristics of the bearing.

Einfluss hydrodynamischer Planetengleitlager auf das NVH-Verhalten von Windenergieanlagen

Zusammenfassung

Das Wachstum des Windenergiesektors wird mit strengen Lärmschutzvorschriften konfrontiert, insbesondere in Bezug auf tonale Geräusche von Windenergieanlagen. Diese tonalen Geräusche, die aus den Vibrationen im Triebstrang resultieren, werden als Körperschall durch die Windenergieanlage übertragen und treten schließlich als Schallemissionen in die Umgebung aus. Da tonale Geräusche für Menschen besonders störend sind, besteht die Notwendigkeit, Maßnahmen zur Reduzierung von NVH bereits in der frühen Entwicklungsphase zu ergreifen.

In letzter Zeit zeichnet sich ein Trend ab, Planetenwälzlager durch Gleitlager in den Getrieben von Antriebssträngen der Windenergieanlage zu ersetzen. Dieser Wechsel bietet mehrere Vorteile, darunter ein geringerer Platzbedarf, eine höhere Zuverlässigkeit und eine verbesserte Reduktion von Vibrationen. Letzteres ist besonders wichtig, um die Lärmschutzvorschriften einzuhalten. Daher zielt diese Arbeit darauf ab, den Einfluss der Verwendung von Planetengleitlagern auf das NVH-Verhalten von Windenergieanlagen zu analysieren. Zu diesem Zweck wird das dynamische Verhalten einer generischen 5-MW-Windenergieanlage unter Nennbetriebsbedingungen mittels eines Mehrkörpersimulationsmodells simuliert. Die Ergebnisse dieser Studie zeigen ein signifikantes Potenzial zur verbesserten Lärmminderung durch den Einsatz von Planetengleitlagern, wobei die Hauptparameter des Lagers eine Rolle in den Dämpfungseigenschaften spielen.

1 Introduction

The wind energy sector has witnessed significant commercial growth over the past decade, with notable commitment from various nations to achieve zero carbon emissions by the mid-21st century [1]. Despite this progress, there exists sustained pressure within the wind industry to reduce the

✉ Moataz Sabry
moataz.sabry@cwd.rwth-aachen.de

[1] Center for Wind Power Drives, RWTH Aachen University, Campus-Boulevard 61, 52074 Aachen, Germany

Published online: 10 February 2025

levelized cost of electricity (LCoE) while also complying with legal limitations concerning sound emission [2, 3].

In one respect, competitiveness characterizes energy markets, with various renewable energy sources, including wind, competing to offer the most cost-effective electricity. To achieve lower LCoE, WTs are to be designed with larger rotor diameters to achieve higher power ratings while also featuring more compact drivetrains to reduce costs [4]. This leads to higher rotor hub load that the drivetrain must sustain. Hence, there is a continuous demand for improvement in drivetrain component design in terms of power density. A notable trend in recent years involves replacing conventional rolling element bearings (RBs) used as planet gear bearings in WT gearboxes with journal bearings (JBs). This shift is driven by the advantages of JBs, including reduced installation space, higher reliability, and enhanced vibration reduction [6], the latter being particularly crucial for adhering to noise regulations.

In the other respect, the wind energy sector faces increasingly stringent noise protection regulations [2]. Those regulations define the minimum distance required of a wind turbine to urbanized areas. Noncompliance with these noise protection regulations can have significant consequences for the WT operation, ranging from startup delays to suboptimal operation modes with reduced aeroacoustic noise emission and power output. In extreme cases, even the decommissioning of WTs can be a consequence, posing substantial economic risks to operators. In this regard, a major concern is the tonal noise generated by WT drivetrains. In comparison to the broadband noise generated by WTs blades, tonal noise is often perceived as more irritating by human recipients.

These tonalities primarily arise from periodic vibrations in the drivetrain [7], such as those caused by gear meshing or the electro-mechanical excitations from the generator. These vibrations are transmitted as structure-borne sound through the WT machinery, eventually reaching the outer surface of the WT, for example, the rotor blade surface [8]. At this point, the vibrations are radiated as airborne sound into the surrounding environment, where they are perceived by nearby residents [9, 10].

Given the relevance of the NVH behavior of WTs, particularly tonalities, addressing this issue during the early stages of drivetrain development is crucial. While field and test rig measurements are commonly used for this purpose, they are costly and may prolong the development cycle due to the need for prototype construction. In contrast, numerical investigations offer a more efficient and faster assessment, as they allow for versatile and customizable testing of different WT designs regarding NVH behavior through simulations. This makes them well-suited for early-stage development. Nonetheless, accurately modeling the dynamic behavior of mechanical components can still be challenging [11].

Several studies have explored the NVH behavior of WTs through numerical analysis, investigating system-level aspects such as the effects of various drivetrain configurations [12]. Other studies have focused on specific components, such as the influence of RBs [8, 13] or excitation forces generated by the generator of direct-drive WTs [14]. Nevertheless, research on the impact of JBs on NVH behavior of WT remains limited. To the authors' knowledge, the numerical and experimental studies conducted by [8, 15–17] have explored this aspect to some extent. While some investigations included PJBs, others focused on JBs in different drivetrain areas, such as for the sun gear of the high-speed shaft (HSS).

Experimental studies conducted by Meyer et al. demonstrated the successful operation of a gearbox prototype equipped with JBs in both test rigs and field conditions. Their findings indicate that JBs can operate hydrodynamically under wind power-specific conditions, resulting in benefits such as reduced structure-borne sound vibrations [16, 17].

Vanhollebeke et al. investigated mechanical noise originating from gearbox bearings using a multi-body gearbox model where the bearings were represented through stiffness and damping values. Their research showed that replacing RBs with JBs significantly improved the overall noise and vibration behavior. The damping values of the bearings were determined by linearizing the lubricant pressure field distribution of the JBs under their operating conditions, underscoring the importance of conducting EHD simulations to obtain the lubricant state as a primary step. Additionally, experiments on a test rig, where a gearbox prototype was refitted with JBs, revealed a significant reduction in vibration amplitudes compared to RBs [8].

Siddiqui et al. investigated the dynamic behavior of a WT gearbox with RBs and JBs used as the HSS bearing. Their simulations observed significant damping of HSS vibrations in the JB based gearbox model. Furthermore, the authors emphasize the need for further research focused on studying the interactions between the gearbox and JBs, alongside a detailed WT model [15].

Thus far, a complete understanding of the influence of PJBs on the NVH behavior of WTs remains unknown. For this purpose, a comprehensive MBS WT model featuring PJBs is required. Determining the NVH-relevant parameters needed to model the PJBs, particularly stiffness and damping coefficients, presents a significant challenge. In the case of RBs, modeling these parameters in an NVH model is often done through a single load-displacement curve. For JBs, however, these parameters vary considerably depending on the lubricant film pressure. The pressure itself varies

across the bearing surface and is highly dependent on the operating conditions of the bearing [6].

Detailed EHD simulations can address this complexity by obtaining the lubricant film state during operation through solving the Reynolds equation [18]. Although computationally more intensive than a simplified linearized model and particularly in combination with a comprehensive MBS WT model, EHD simulations enable more accurate assessments of the influence of these bearings on the WT NVH behavior.

Therefore, this study aims to investigate the NVH characteristics of PJBs and their impact on the NVH behavior of WTs, focusing on system dynamics and potential tonalities. This objective is pursued through a combination of an MBS WT model featuring EHD simulations to comprehensively model the dynamic behavior of a generic 5 MW WT featuring PJBs under nominal operating conditions. By analyzing various frequency response functions (FRFs) between two selected points in the drivetrain, the study assesses when and to what extent the PJBs contribute to the propagation of structure-borne sound to the WT outer surfaces. This assessment includes comparisons with PRBs and considers variations in the PJBs' main parameters, namely bearing clearance, width-to-diameter ratio, and lubricant viscosity.

2 Modelling approach

The characteristics of this MBS model will be presented in this section. The discussed model was originally developed at the Chair for Wind Power Drives [12], but has been slightly adjusted to feature PJBs for the purposes of this study.

The MBS model employed in this study is depicted in Fig. 1. The figure provides a closeup view of the key components of the WT drivetrain. In this model, the main shaft is supported by two main bearings (tapered rolling bearings) fixed to the drivetrain housing, which is, in turn, connected to the machine frame via four spring-damper elements. On the upwind side, the main shaft is rigidly connected to the rotor hub, and on the downwind side, to the low-speed shaft (LSS) gearset.

The planetary carrier of the LSS gearset incorporates five helical planet gears supported by PJBs. The ring gear

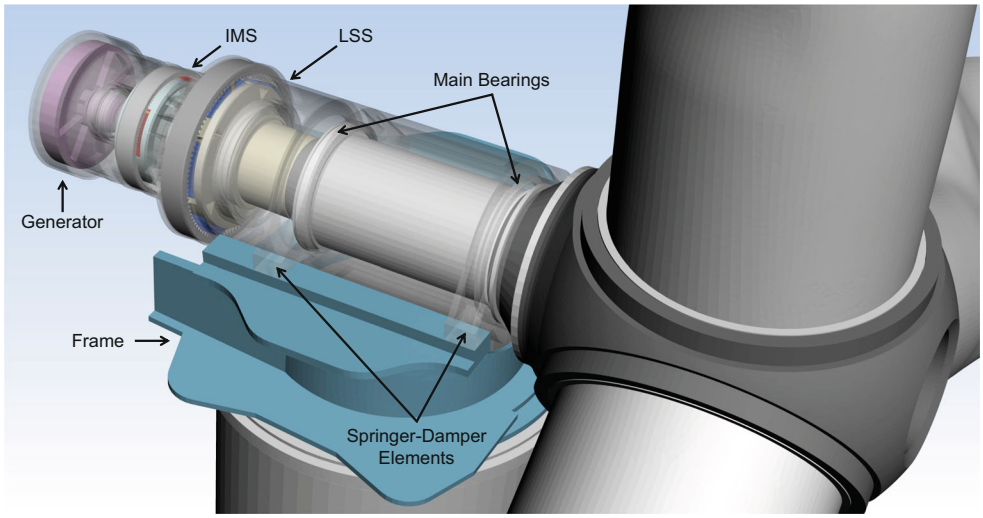

Fig. 1 MBS model of the 5 MW WT equipped with PJBs in the LSS gearset

Table 1 Gearbox parameters

Parameter	Symbol	Gearset		Unit
		LSS	IMS	
Transmission ratio	i	4.33	6.52	[–]
Module	m	25	14	[mm]
Helix angle	β	10	8	[°]
# Sun teeth	z_1	30	23	[–]
# Ring teeth	z_2	–100	–127	[–]
# Planet teeth	z_p	35	52	[–]
# Planets	N_p	5	3	[–]
JB width	W	380	–	[mm]
JB diameter	D	300	–	[mm]
JB clearance	ψ	0.5	–	[‰]

is clamped into the drivetrain housing and remains non-rotatable, while the sun gear is mounted on the intermediate shaft (IMS). The IMS gearset features three helical planet gears, which are supported by the typical PRBs on the carrier. As with the LSS gearset, the ring gear is clamped into the drivetrain housing, and the sun gear, as the output, is mounted on the generator shaft.

In this configuration, the drivetrain features a two-stage planetary gearbox, which is typical for integrated drivetrains. For simplicity and to reduce computational costs, PJBs are included only in the LSS gearset. Unlike the IMS, the LSS is subjected to the full rotor torque, making it the primary choice to benefit from the increased power density offered by PJBs.

The LSS gearset and its PJBs are designed according to the current state of the art of PJBs in WTs [17], aiming for hydrodynamic operation of the JBs under the nominal operating conditions of a 5 MW WT. The parameters for the LSS gearset and its JBs, as well as those for the IMS gearset, are detailed in Table 1.

Excitations from gear meshing are significant sources of vibration in WT drivetrains. Therefore, comprehensive gear modeling is essential to accurately simulate these sources. This study employs a force element model to simulate tooth mesh interactions, considering factors such as gear distance, position, and orientation. Gear misalignment effects are addressed to account for profile modifications and tilt, the latter being crucial for accurately describing the dynamic behavior of the planet gear and its JB [19, 20]. Contact forces, including stiffness, damping, and friction, are calculated using the 'Weber/Banaschek' approach [22]. Additionally, gear flexibility is incorporated into the model, further enhancing the NVH assessment of the WT.

The LSS PJBs are modeled using a force element, which simulates lubricated conformal contact between two bearing surfaces by solving the Reynolds equation [18]. This approach facilitates the analysis of various bearing performance characteristics, including forces, pressure distribution, and relative eccentricity. In this study, EHD simulations are conducted, considering the local flexible deformation of both bearing surfaces and their influence on oil film height h. For the sake of simplicity, the calculation of bearing temperature and its influence on lubricant viscosity, as well as the effect of surface roughness on bearing hydrodynamics, are not addressed in this study.

The five JBs are equipped with grooves according to DIN 7477 to supply lubricant. A lubricant of viscosity class ISO VG 320 at a nominal temperature of 60 °C is used in this study, as it is commonly employed in WTs [17]. Additionally, a simple quadratic profile (Fig. 2) is applied to the surface of the bearing sleeve to manage the elevated bearing pressures at the edges caused by planet gear tilt [19]. In the equation, x, φ, ψ, R, W represent the bearing's axial and circumferential coordinate, dimensionless clearance, radius, and width, respectively.

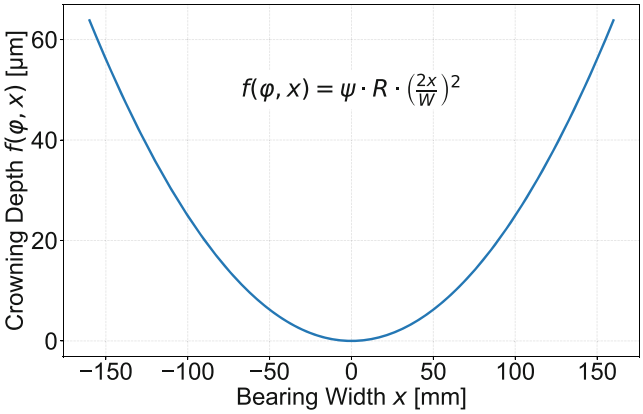

Fig. 2 Crowning profile applied to the PJBs

To compare the influence of PJBs with PRBs, a comprehensive force element is required to accurately describe the dynamic behavior of RBs. This force element enables the detailed calculation of forces and torques transmitted by RBs, considering their geometric properties in accordance with ISO 16281. The calculation is performed for each rolling element and accounts for nonlinear stiffness characteristics, as well as clearance and cross-coupling effects, using the lamina roller model [21]. The damping characteristics are calculated based on the assumption of constant natural damping. In this work, a standard cylindrical RB from the catalog is selected, featuring the same inner ring diameter as the JB but with half the width. Consequently, two RBs placed side by side are used to support each planet gear, replacing the single JB.

The generator is not extensively detailed here; only the rotor wheel of the generator is included as part of the output shaft. The generator torque is applied to the rotor using a concentrated load approach. This simplification overlooks the reality where the airgap forces are distributed among the airgap surface of the rotor and stator [14]. Consequently, torque ripples and other excitations from the generator are neglected, leaving the gears meshing as the primary noise source in the model.

Furthermore, the nacelle cover of the WT is neglected as well, as it is irrelevant to the investigation of structure-borne sound transfer within the drivetrain [23], which is the focus of this study. The wind-dependent azimuth and pitch bearings have their movement restricted, as wind effects are not considered. Instead, the rotor hub is constrained to rotate at a nominal speed of 10 rpm under the nominal operating conditions of a 5 MW WT.

The drivetrain components are modeled as flexible structures. The geometries of all components are imported into a finite element (FE) environment (Fig. 3), where they are meshed and associated with material parameters. The

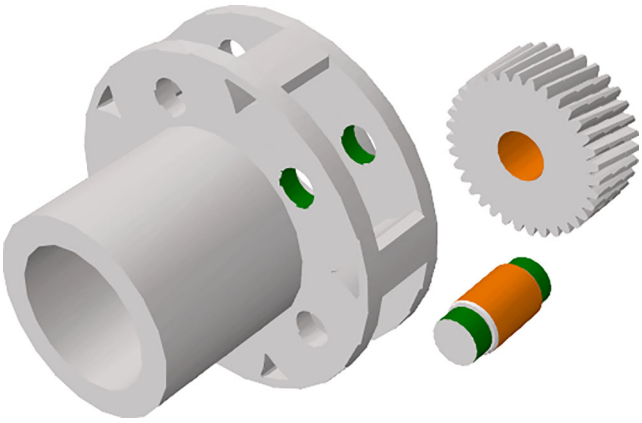

Fig. 3 FE models of the LSS gearset: orange indicates EHD surfaces, and green represents tie constraints

carrier is represented using EN-GJS-700-2, while the pin sleeve is modeled using CuSn12Ni2-C. All the gears are modeled using 18CrNiMo7-6. Modal reduction is then performed according to the Craig-Bampton method [7]. Selected Degrees of Freedom (DOFs) are identified as Master-DOFs to introduce loads at the corresponding locations in the MBS.

To conduct the NVH analysis, it is necessary to determine excitation and measurement points, between which transfer functions (FRFs) can be computed. This approach is used to assess how much the oil film in the PJBs contributes to the propagation of structure-borne sound to the outer surfaces of the WT. As in Fig. 4, sensors are placed in the WT model that measure body acceleration concentric at the following locations: tower top and rotor hub. These locations are selected because they serve as key interfaces with the tower and rotor blades, where significant sound emissions from the WT are anticipated [23]. The excitation point lies at one of the five planet gears.

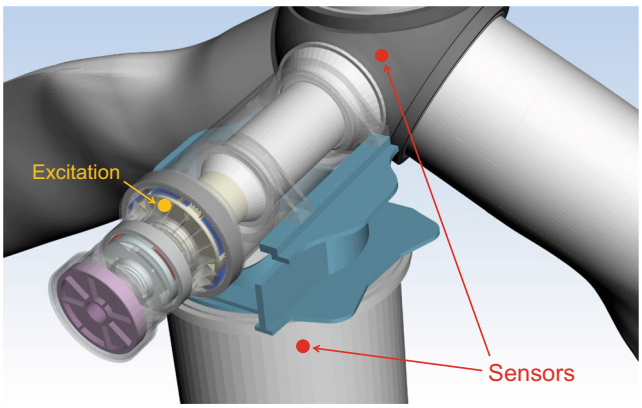

Fig. 4 Placement of the excitation and sensor points in the WT model

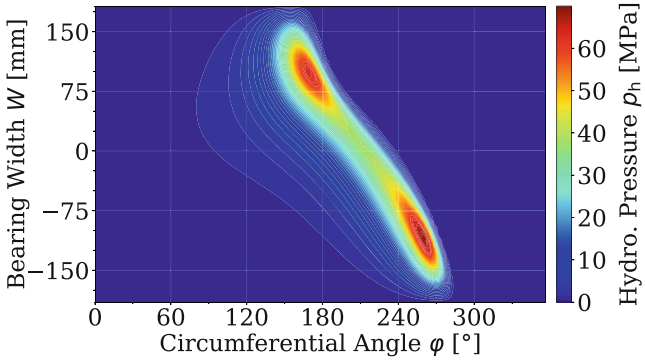

Fig. 5 Hydrodynamic pressure field of PJBs during nominal operating conditions

3 Results & discussion

During nominal operating conditions (5 MW and 10 rpm), the PJBs slide at a rotational speed of approximately 0.45 m/s and exhibit an average bearing pressure of 10.2 MPa. The hydrodynamic pressure field distribution across the PJB surface is illustrated in Fig. 5. The two prominent high-pressure zones observed at the bearing ends, with an angular separation of approximately 180°, are characteristic of planetary bearings.

Under rated operating conditions, the PJBs exhibit no asperity contact, attributable to the applied quadratic profile to the bearing surface. Without this profile, the high-pressure zones exhibit even higher hydrodynamic pressure values and additional contact pressure due to asperity contact. Over the course of one full rotor rotation, the maximum hydrodynamic pressure during operating conditions is approximately 90 MPa, which is significantly below the yield strength of the pin sleeve material, approximately 180 MPa, indicating a safety margin in its hydrodynamic carrying capacity.

Prior to exploring the various FRFs of the WT model, it is beneficial to understand the excitations originating from the drivetrain using spectrograms. This understanding aids in identifying potential tonalities and the frequency regions where most of the excitation frequencies are located. Consequently, when analyzing the FRFs, focus can be directed to this region.

The spectrograms of absolute accelerations obtained from the sensor at the rotor hub of the WT model, equipped with PJBs and PRBs in the LSS gearset, are presented in Fig. 6. For these spectrograms, a 50-second ramp-up simulation is conducted for both model variants to obtain the excitation frequencies dependent on rotor rotational speed.

The vertical red line represents the nominal rotor rotational speed of the WT. The more prevalent but less intense rays represent the gear mesh frequency and its upper harmonics $f_{\mathrm{LSS},i}$ arising from the LSS gearset. The more intense

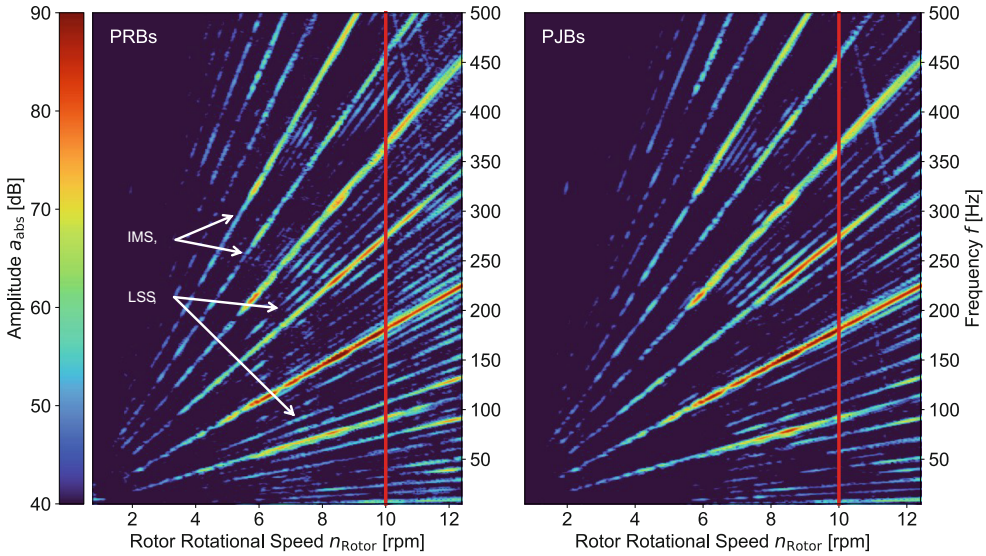

Fig. 6 Spectrograms of absolute accelerations obtained at the rotor hub of the WT model, equipped with PRBs (left) and PJBs (right) in the LSS gearset

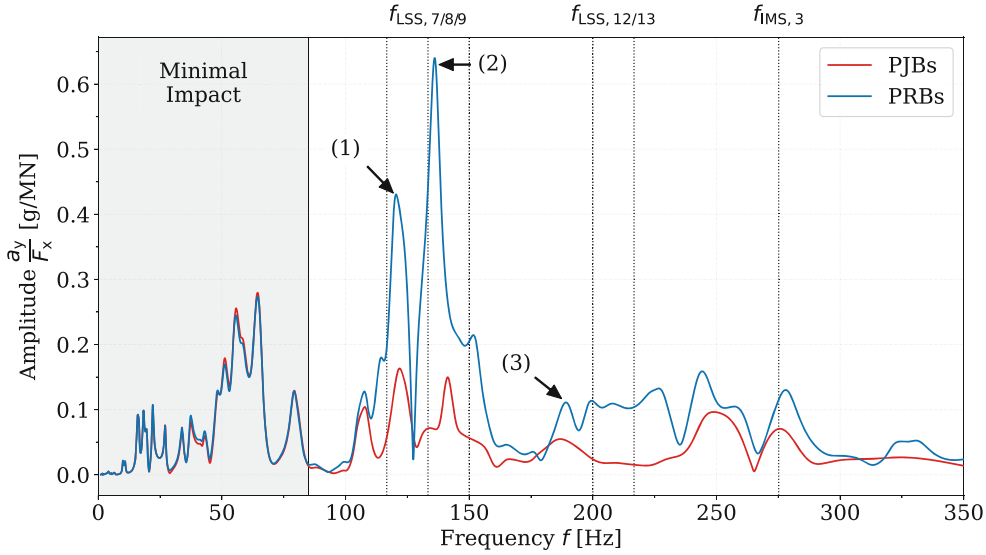

Fig. 7 FRFs resulting from an excitation at the LSS planet gear in the x direction and the acceleration response at the tower top in the y direction

but less prevalent rays represent the gear mesh frequency and its harmonics $f_{IMS,\,i}$ of the IMS gearset. The gear mesh frequencies at the nominal rotor rotational speed are summarized in Table 2.

From the figure, it can be observed that the WT model with PJBs generally exhibits reduced dB levels. This reduction is particularly noticeable for the mesh frequency harmonics of the LSS gearset, averaging approximately 2.7 dB lower at the rotor hub for the LSS excitation frequencies. A reduction of about 1.5 dB is also observed at the towertop.

Table 2 Gear mesh frequencies of the WT model gearbox at nominal rotor rotational speed

Stage	Gear Mesh Frequency (10 RPM)
LSS	16.66 Hz
IMS	91.72 Hz

The frequency harmonics of the IMS gearset remain largely unaffected. This is expected, as only the bearings in the LSS gearset are changed. In what follows, the study concentrates on frequencies up to 350 Hz, as, beyond this range, the excitation intensity from the LSS gearset diminishes for both model variants, and no more significant system resonances appear in the various FRFs.

To analyze the difference in transfer behavior between the two bearing variants, the amplitude curve of two FRFs—resulting from an excitation at the LSS planet gear in the x direction and the acceleration response at the tower top in the y direction—is illustrated in Fig. 7. It is computed for the WT model with either PJBs or PRBs in the LSS gearset.

Minimal differences in transfer behavior between PJBs and PRBs are observed up to approximately 80 Hz. This phenomenon is also noticeable in other FRFs obtained at

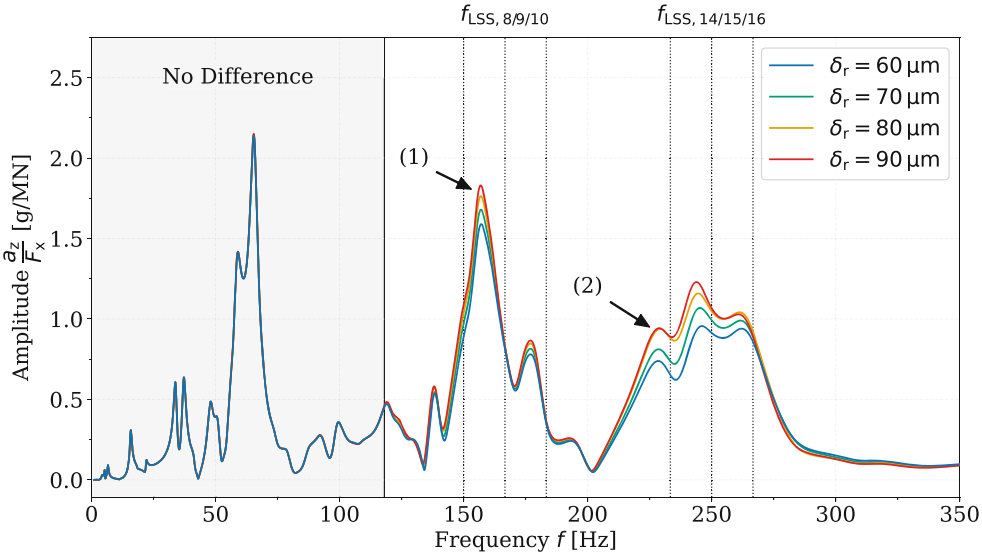

Fig. 8 FRFs resulting from an excitation at the LSS planet gear in the z direction and the acceleration response at the tower top in the x direction

the rotor hub or blade tip for different acceleration directions. This can be attributed to the vibration characteristics of the WT in this frequency range, where the LSS gearset does not exhibit a significant vibration pattern within the overall drivetrain vibration pattern. Instead, it mainly oscillates rigidly with the entire drivetrain.

Consequently, there is minimal oscillation within the LSS gearset in this frequency range, where the planetary bearings could exert influence. Starting at approximately 100 Hz, the participation of the LSS gearset in the overall drivetrain oscillations becomes evident, particularly in the WT model with PJBs. This model exhibits reduced responses with damped resonance peaks in the amplitude curve of the FRFs. This is notably observed at two resonance peaks: (1) around 120 Hz, primarily representing a whirling vibration mode about the drivetrain axis, and (2) at 136 Hz, corresponding to a higher-order lateral bending mode. The use of PJBs results in a reduction in vibration amplitude of approximately 8 and 12 dB, respectively, for these two resonance peaks and this combination of measurement and excitation directions.

Analysis of the FRF amplitude curves reveals differences in system stiffness between the two bearing types. The FRF amplitude for the WT model with PJBs shows a slight rightward shift, indicating increased stiffness at corresponding frequencies for this transfer combination of measurement and excitation point. For example, the resonance frequency (1) shifts slightly to the right for the WT model with PJBs. However, at resonance peak (3) around 189 Hz, the response for the WT model with PJBs appears less stiff but more damped. Despite these observations, the overall stiffness of the system shows minimal variation, suggesting that the impact of PJBs on the total stiffness of the system is negligible compared to the impact on the system damping.

Vertical dotted lines in Fig. 7 denote relevant excitation frequencies at the rotor's nominal rotational speed, resulting from the gear meshing of the LSS and IMS gearsets observed in Fig. 6. These frequencies are located near resonance peaks and contribute to tonalities. In such cases, the response may be better damped by opting for PJBs.

To further understand the impact of PJBs on the NVH behavior of WTs, bearing parameters are to be examined, such as the bearing clearance δ_r. Figure 8 presents the amplitude curves of various FRFs resulting from excitation at the LSS planet gear in the x direction and the acceleration response at the tower top in the z direction. These FRFs are calculated for different radial clearance values δ_r in the PJBs.

As already observed in Fig. 7, there exists no significant impact on the lubricant film's transfer up to approximately 120 Hz. This further suggests minimal oscillation within the LSS gearset in this range, where the bearings might exert influence. Beyond 120 Hz, increasing the bearing radial clearance leads to reduced damping and more pronounced resonance peaks. This effect is especially notable at the following resonance frequencies: (1) around 156 Hz, associated with lateral and vertical bending modes of the drivetrain, and (2) approximately 226 Hz, related to the vertical bending mode of the main shaft combined with the lateral bending mode of the drivetrain. This results in an average increase in vibration amplitude of 0.75 dB per 10 µm increase in bearing clearance δ_r at these resonance peaks.

Analysis of the FRF amplitude shows minimal changes in system stiffness with varying bearing radial clearance δ_r. Although resonance peaks may shift slightly with increased clearance—rightward at (1) and leftward at (2)—overall stiffness remains largely unaffected. In contrast, damping characteristics exhibit more noticeable changes.

Table 3 Influence of the PJB design parameters on the transfer behavior of the lubricant film, "○" represents no change; "–" indicates a decrease, while "+" indicates an increase

Increase in		Stiffness	Damping
Radial clearance	δ_r	○	–
Lubricant viscosity	η	○	+
Width-Diameter ratio	W/D	○	+

Vertical dotted lines in the figure indicate excitation frequencies at the rotor's nominal rotational speed, resulting from the meshing of the LSS gearset. These excitation frequencies are closely aligned with resonances that could potentially lead to resonance issues and may be better damped with smaller bearing clearances δ_r. While these excitation frequencies may not exactly match the resonance frequencies, they could align with resonance frequencies if the WT operates at a rotational speed slightly different from its rated speed.

In this study, further JB main design parameters are examined, and the impact of increasing the value of the bearing main parameters on the system's stiffness and damping is summarized in Table 3. The results indicate that all examined parameters have negligible influence on stiffness but do affect the damping behavior of the bearing.

4 Conclusion

In this study, the impact of a LSS gearset with PJBs on the NVH behavior of a 5 MW WT is examined. This analysis involves comparing the spectrograms and transfer characteristics of PJBs with those of PRBs, as well as varying several JB parameters, such as bearing clearance. A comprehensive MBS model of a 5 MW WT is utilized for this purpose. The spectrograms and FRFs indicate that a WT equipped with PJBs generally produces lower noise levels. While the initial frequency responses for both bearing types are similar, JBs exhibit superior damping and reduced resonance peaks at higher frequencies. Additionally, the study shows the effects of changes in lubricant viscosity, bearing width ratio, and clearance on transfer characteristics. It is found that increased viscosity and bearing width enhance damping, whereas increased clearance adversely affects damping. The influence on system stiffness is found to be negligible.

Future research should investigate the simultaneous effects of various design parameters on the transfer characteristics of oil films. The optimal combinations of parameters, such as bearing clearance and lubricant viscosity, for achieving optimal damping remain unclear due to nonlinear interactions.

Additionally, other factors, including asperity contact, bearing surface roughness, different crowning profiles, oil groove placement, or thermal effects, could also be examined. Some of which can be estimated based on the results of already tested ones. For example, thermal effects are expected to influence the system similarly to viscosity variations. However, asperity contact introduces notable differences. In a PJB operating in the mixed-lubrication regime, vibrations are transmitted not only through the lubricant but also via asperity contact, which has lower damping properties, leading to reduced vibration mitigation.

Acknowledgements The authors would like to thank the German Federal Ministry for Economic Affairs and Climate Action for the financial support. They also extend their gratitude to their project partners for the insights into the equipment and the expertise provided, both of which contributed to this joint project.

Federal Ministry
for Economic Affairs
and Climate Action

Funding Open Access funding enabled and organized by Projekt DEAL.

Conflict of interest M. Sabry, G. Jacobs, T. Decker, W. Schünemann and R. Schelenz declare that they have no competing interests.

References

1. (2022) GWEC: wind turbine suppliers see record year for deliveries despite supply chain and market pressures. https://gwec.net/windturbine-suppliers-see-record-year-for-deliveries-despite-supply-chain-and-market-pressures/
2. (2002) Bundes-Immissionsschutzgesetz: Maschinenlärmschutzverordnung. BGBl I:3478

3. Daners D, Nickel V (2021) More torque is better than torque: higher torque density for gearboxes. In: Conference for wind power drives, vol 20
4. Roscher B (2020) Multi-dimensionale windparkoptimierung in der planungsphase: multi-dimensional wind farm optimization in the concept phase. Verlagsgruppe Mainz, Aachen
5. Vázquez-Hernández C, Serrano-González J, Centeno G (2017) A market-based analysis on the main characteristics of gearboxes used in onshore wind turbines. Energies 10(11):1686
6. Lubenow K, Schuhmann F, Schemmert S (2019) Requirements for wind turbine gearboxes with increased torque density with special attention to low-noise turbine operation. In: Conference for wind power drives, pp 3–21
7. Drichel P, Jaeger M, Müller-Giebeler M (2019) Mit elektrischem Antrieb und modellbasierter Systemanalyse nahezu lautlos in die Zukunft. ATZextra 24(5):52–57
8. Vanhollebeke F, Peeters J, Vandepitte D, Desmet W (2015) Using transfer path analysis to assess the influence of bearings on structural vibrations of a wind turbine gearbox. Wind Energy 18(5):797–810
9. Schneider L, Hanus K (2017) Origin, transfer, and reduction of structure-borne noise in wind turbines. In: Proceedings of the 7th international conference on wind turbine noise. The Netherlands, Rotterdam, pp 2–5
10. Grätsch T, Zarnekow M, Ihlenburg F (2019) Simulation of sound radiation of wind turbines using large-scale finite element models. In: Wind turbine noise 2019: international conference on wind turbine noise
11. Lund J, Thomsen K (1978) A calculation method and data for the dynamic coefficients of oil-lubricated journal bearings. In: Topics in fluid film bearing and rotor bearing system design and optimization
12. Schünemann W, Schelenz R, Jacobs G (2023) Comparison of transfer path characteristics for different wind turbine Drivetrain variations. Forsch Ingenieurwes 87(1):139–145
13. Xu Z, Mei X, Wang X, Yue M, Jin J, Yang Y, Li C (2022) Fault diagnosis of wind turbine bearings using a multi-scale convolutional neural network with bidirectional long short-term memory and weighted majority voting for multi-sensors. Renew Energy 182:615–626
14. Duda T, Mülder C, Jacobs G, Hameyer K, Bosse D, Cardaun M (2021) Integration of electromagnetic finite element models in a Multibody simulation to evaluate vibrations in direct-drive generators. Forsch Ingenieurwes 85(2):257–264
15. Siddiqui MO, Chodvadiya A, Luo J (2023) The influence of journal bearings on the gearbox dynamics of a 5-MW wind turbine Drivetrain. J Phys: Conf Ser 2626:12009
16. Meyer T (2015) Design of Journal Bearings for Wind Turbine Gearboxes and Their Validation. In: Conference for Wind Power Drives, CWD 2015: Conference Proceedings. Aachen, Germany
17. Meyer T (2017) Journal bearings in wind turbines: extended investigations for reliability. In: HMI MDA forum. Hannover
18. Reynolds O (1886) On the Theory of Lubrication and Its Application to Mr. Beauchamp Tower's Experiments, Including an Experimental Determination of the Viscosity of Olive Oil. Philos Trans Royal Soc Lond 177:157–234
19. Hagemann T, Ding H, Radtke E, Schwarze H (2021) Operating behavior of sliding planet gear bearings for wind turbine gearbox applications—part I: basic relations. Lubricants 9(10):97
20. Hagemann T, Ding H, Radtke E, Schwarze H (2021) Operating behavior of sliding planet gear bearings for wind turbine gearbox applications—part II: impact of structure deformation. Lubricants 9(10):98
21. Harris TA, Kotzalas MN (2006) Advanced concepts of bearing technology: rolling bearing analysis. CRC Press
22. Niemann G, Weber C, Banaschek K (1953) Formänderung und Profilrücknahme bei Gerad- und Schrägverzahnten Rädern. Schriftenreihe Antriebstechnik. Vieweg
23. Cardaun M, Mülder C, Decker T, Dilba B, Duda T, Schelenz R, Jacobs G, Hameyer K, Keuchel S (2022) Multi-physical simulation Toolchain for the prediction of acoustic emissions of direct drive wind turbines. J Phys: Conf Ser 2265:42047